11th Australasian Fluid Mechanics Conference
University of Tasmania, Hobart, Australia
14-18 December 1992

NUMERICAL SIMULATION OF LOW Pr UNSTEADY NATURAL CONVECTION

P.G. ESPOSITO[1] and M. BEHNIA[2]

[1]INSEAN, Via di Vallerano 139, 00128 Roma, ITALY

[2]School of Mechanical & Manufacturing Engineering, University of NSW, Kensington, NSW 2033, AUSTRALIA

ABSTRACT

A numerical study of natural convection of low Prandtl number liquids is undertaken. An accurate time marching technique has been used to simulate steady and unsteady flows. Results have been obtained for the two-dimensional case over a range of Prandtl and Grashof numbers. Limited results for the three-dimensional case are presented and compared with the two-dimensional simulations.

INTRODUCTION

The problem of thermally-driven convection of low Prandtl number fluids (i.e. liquid metals) is relevant to a wide range of engineering and industrial applications such as material processing, crystal growth, manufacturing and welding. For example, in crystal growth, the flow structure and thermal field play a very important role on the crystal formation and quality (Hurle, 1983 and Langlois, 1985). The study of these types of flows also allows a better understanding of the behaviour of nonlinear dynamic systems, in fact, it is well known that as buoyancy increases (i.e. at larger Grashof numbers), there is a transition from a steady flow to an unsteady oscillatory one (Roux, 1990). This oscillatory instability is associated with a Hopf bifurcation which significantly changes the flow structure. At higher values of the Grashof number there is also a reverse transition from the oscillatory flow to a steady one (Behnia et al. 1990).

The problem is further complicated by the three-dimensionality effects which can strongly affect the flow and the thermal structures (Behnia and de Vahl Davis, 1990; Afrid and Zebib, 1990). In studying this problem, experimental techniques such as Laser Doppler Velocimetry (LDV) cannot be used because the media is opaque and the introduction of measuring probes into the flow not only causes interference but also may yield erroneous measurements because of the non-wetting nature of these liquids. For these reasons, in an experimental investigation of these flows, at best only global quantities, like the average Nusselt number can be measured. To this end, a computational approach to the problem becomes very attractive as it enables one to obtain a detailed picture of the flow pattern and its evolution in time. However, it is noted that because of the low Prandtl number values, the inertial forces are dominating with viscous effects confined in very thin regions near the wall and hence the problem becomes very non-linear. Therefore it is essential that the numerical algorithms are fast, efficient and robust. Further, the unsteady nature of the problem requires very accurate time discretization, otherwise very erroneous results may be obtained.

The work presented here is concerned with the transient numerical simulation of the buoyancy driven convection of a liquid metal in an enclosure. A very accurate finite difference based algorithm is used to obtain results both in two and three dimensional geometries. The two dimensional results are compared with those of Mohamad and Viskanta (1991).

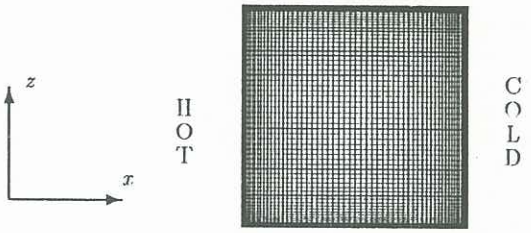

Figure 1: Two dimensional 64 × 64 grid.

GOVERNING EQUATIONS

An upright cavity of unity aspect ratio is considered. The motion of the Boussinesq fluid is due to the buoyancy force generated by the temperature difference between the two isothermal hot and cold vertical walls. The other walls are assumed to be adiabatic. All walls of the enclosure are solid impermeable and stationary. The problem is defined by the continuity, Navier–Stokes and energy equations. They are nondimensionalised using the appropriate scalings of ΔT (temperature difference between the hot and cold wall), L (cavity width), L^2/α (diffusion time) and α/L (velocity). In the nondimensional form the equations are:

$$\nabla \cdot \mathbf{v} = 0 \tag{1}$$

$$Pr^{-1}\left(\frac{\partial \mathbf{v}}{\partial \tau} + \nabla \cdot (\mathbf{v}\mathbf{v})\right) = -Pr^{-1}\nabla P + \nabla^2 \mathbf{v} - Ra\theta\hat{\mathbf{k}} \tag{2}$$

$$\frac{\partial \theta}{\partial \tau} + \nabla \cdot (\mathbf{v}\theta) = \nabla^2 \theta \qquad (3)$$

where $\mathbf{v} = U\hat{\mathbf{i}} + V\hat{\mathbf{j}} + W\hat{\mathbf{k}}$, P is the pressure, θ is the temperature field, $Pr = \nu/\alpha$, $Ra = GrPr = g\beta L^3 \Delta T/\nu\alpha$. The initial conditions are assumed to be that the fluid is at rest and at the cold wall temperature:

$$\mathbf{v} = 0 \qquad (4)$$

$$\theta = 0 \qquad (5)$$

Then suddenly the hot wall temperature is increased to unity initiating the flow. At the boundaries the conditions are:

$$\theta = 1 \quad \text{at } x = 0 \qquad (6)$$

$$\theta = 0 \quad \text{at } x = 1 \qquad (7)$$

$$\frac{\partial \theta}{\partial n} = 0 \quad \text{on all other walls} \qquad (8)$$

$$\mathbf{v} = 0 \quad \text{on all walls} \qquad (9)$$

NUMERICAL SCHEME

The governing equations are discretized using finite difference approximations; a second order centered scheme is used for the space discretization. Because of the sharp gradients of physical quantities it is essential to use non-uniform grid spacings. The grid is generated using sine functions, which allowed very fine grid spacings near the walls becoming gradually coarser away from them. A typical 64×64 grid used in the two dimensional computations is shown in Fig. 1.

The diffusion terms are discretized in time by means of an implicit Crank-Nicholson method. For the convective terms of the equations a conservative form is used.

A low-storage Runge–Kutta method (Wray, 1987) is adopted for the time marching procedure. The solution at the new time step is obtained using three sub-steps; in each sub-step a fractional step method (Kim and Moin, 1985) is used. The time discretization technique provides an overall accuracy of the second order. Because of the implicit treatment of the diffusion terms, the constraint on the time step size is reduced; in fact, this is only limited by the Courant-Friedrichs-Levy stability condition of $CFL \leq \sqrt{3}$. In the primitive variable formulation of the Navier–Stokes equations, the evaluation of pressure requires the solution of an elliptic equation. Since a direct solver is not suitable for a three dimensional problem, a Correction-Storage multigrid is used to speed up the convergence rate of an iterative solver (Brandt, 1977 and Esposito, 1991).

RESULTS

For testing and comparison purposes, initially two dimensional results were obtained. Also, some three-dimensional flow calculations were carried out. The results which have been generated so far are as follows.

Two Dimensional Case

For this case we chose three different values of Prandtl number ($Pr = 0.001$, 0.005, 0.01). For comparison purposes, the range of parameters was close to that of Mohamad and Viskanta (1991). A mesh sensitivity analysis was performed using three different grids (32×32, 64×64 and 128×128). For the case of $Pr = 0.005$ and $Gr = 10^7$, solutions at the same time were compared. It was noted that the solutions generated using 64×64 and 128×128 cells were extremely close. Therefore, as a compromise between accuracy and computational cost, the 64×64 grid was selected. In fact, the coarser grid (32×32) solution also showed the features of the flow quite accurately. This is in line with the observation of Mohamad and Viskanta (1991).

Pr	Gr	Nu	frequency
0.001	10^6	1.0813	steady
	3×10^6	1.2763	2.4
0.005	10^6	1.5996	steady
	2×10^6	1.8975	6.8
	3×10^6	2.0730	8.5
	5×10^6	2.3158	13.7
	10^7	2.6408	17.8
0.01	5×10^6	2.7859	21.0
	10^7	3.1671	25.4

Table I: Summary of two-dimensional results

$Pr = 0.001$ For this value, the stability constraints allowed a time step of $\Delta\tau = 0.001$. Computations were performed at $Gr = 10^6$. The time history of different features of the flow, such as wall Nusselt number, velocity components and temperature at several locations were checked. The solution converged towards a steady state very slowly and after about 10000 time steps the amplitude of the oscillations nearly vanished. The flow primarily comprised of a single cell circulation in the middle of the cavity (Fig. 2). The temperature field showed a slight deformation compared to the conduction solution, due to the convective circulation (see Fig. 2). The results agree with the solution of Mohamad and Viskanta (1991). They also found a steady solution for this case.

As the Grashof number is increased the flow becomes unsteady. At $Gr = 3 \times 10^6$ the flow exhibits a weak oscillation. The frequency of this oscillation depends on Gr ad Pr. A summary of the features of the solution for this run, as well as other cases is given in Table I. The average Nusselt number on the hot (or cold) wall calculated over several periods is also given. Instantaneous contour maps of the stream-function and isotherms at $\tau = 20$ are shown in Fig. 3. A loss of symmetry in the flow field is observed. This is due to the fact that the initiation of the flow is by a non-symmetrical initial condition. As the flow is unsteady, this lack of centro-symmetry is preserved, however averaging of the solution over a long period yields a symmetrical solution. Loss of symmetry in unsteady natural convective flows has also been observed by others (Le Quéré, 1990).

$Pr = 0.005$ For this value of Pr the time step was the same as before (0.001). The solution at $Gr = 10^6$ was steady, whilst for $Gr \geq 2 \times 10^6$ an oscillatory regime is reached after the initial transient. The time history of the Nusselt number given in Fig. 4 clearly shows this. At this Pr the velocity magnitudes are higher than in the previous case and hence the isotherms indicate a stronger

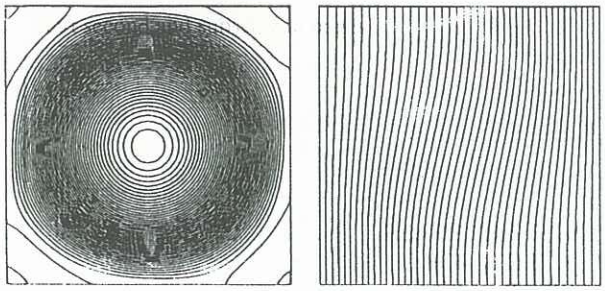

Figure 2: Left: streamlines at $\tau = 10$, $Pr = 0.001$, $Gr = 10^6$; levels $-0.46 \ldots 0.0$ (0.01). Right: temperature field at $\tau = 10$, $Pr = 0.001$, $Gr = 10^6$; levels $0.0 \ldots 1.0$ (0.025)

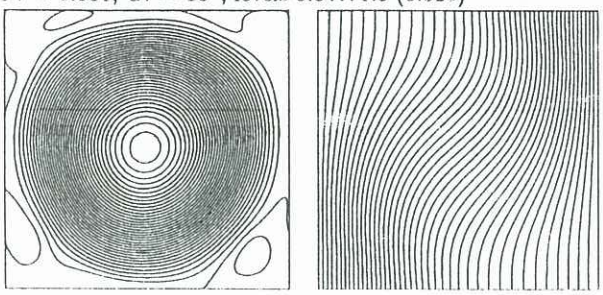

Figure 3: Left: streamlines at $\tau = 20$, $Pr = 0.001$, $Gr = 3 \times 10^6$; levels $-1.80 \ldots 0.05$ (0.05). Right: temperature field at $\tau = 20$, $Pr = 0.001$, $Gr = 3 \times 10^6$; levels $0.0 \ldots 1.0$ (0.025)

departure from the conduction solution. At $Gr = 3 \times 10^6$ the oscillatory flow has a frequency which is more than three times that at $Pr = 0.001$. An increase of Gr leads to a stronger secondary recirculation in the corners of the cavity (see Fig. 5). After the initial transient period, the velocity in the centre of the cavity was recorded and a frequency analysis was performed. For $Gr = 5 \times 10^6$ the amplitude of Fourier transform of the velocity probe time signal is given in Fig. 6. The peak of the first harmonic is clearly shown.

Pr = 0.01 The higher velocities induced by this Pr dictated a smaller time step ($\Delta\tau = 0.0005$). For $Gr = 10^7$ the central cell broke into two, with recirculating cells near the corner (Fig. 7). This transition to multicellular convection agrees with the result of Mohamad and Viskanta (1991).

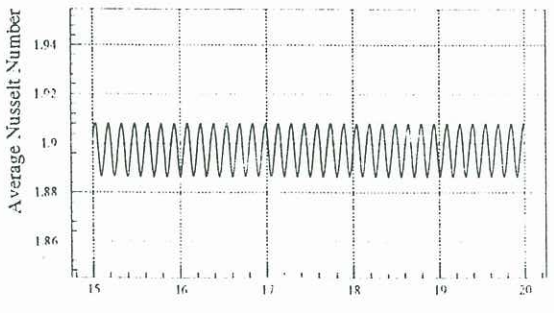

Figure 4: History of the average Nusselt number for $Pr = 0.005$, $Gr = 2 \times 10^6$.

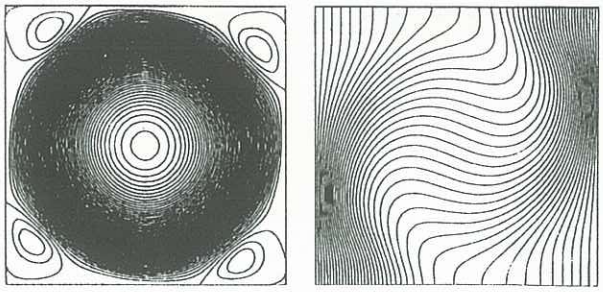

Figure 5: Left: streamlines at $\tau = 10$, $Pr = 0.005$, $Gr = 5 \times 10^6$; levels $-5.9 \ldots 0.2$ (0.1). Right: temperature field at $\tau = 10$, $Pr = 0.005$, $Gr = 5 \times 10^6$; levels $0.0 \ldots 1.0$ (0.025)

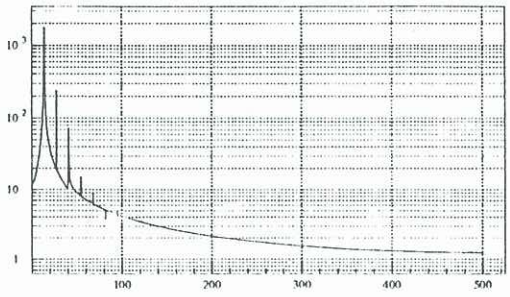

Figure 6: Frequency analysis of a velocity probe time signal; $Pr = 0.005$, $Gr = 5 \times 10^6$

Three Dimensional Case

Due to the excessive 3-D computational cost, so far results have been obtained using a $32 \times 32 \times 32$ grid for lower values of Gr. The CPU time requirement on an IBM RISC/6000-540 for each step was about 10 seconds. Thus it takes more than one day of computation to simulate the evolution of the flow to $\tau = 20$. For $Gr = 10^6$ and $Pr = 0.001$, unlike the two-dimensional solution the flow was unsteady. The three-dimensional unsteady motion was complex and showed that Taylor-Görtler vortex pairs are generated near the solid walls (Fig. 8). As the flow is unsteady and three-dimensional, it is very difficult to visualize it. However, to give a "feel" for the flow structure, we used the velocity field at an instant in time and generated particle tracks. It is noted that these tracks do not represent the correct path of particles and at best just indicate the overall cellular structure of the flow at that time. Fig. 9 shows the flow structure and its three-dimensional nature. Fig. 10 shows velocity oscillations. For this case, the time averaged Nu was 1.19. $Pr = 0.01$ was also simulated. The time history of Nu indicates that the flow is unsteady (Fig. 11).

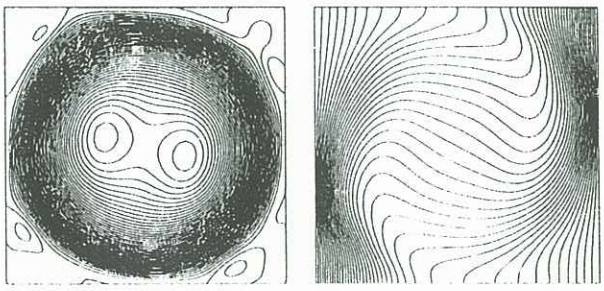

Figure 7: Left: streamlines at $\tau = 10$, $Pr = 0.01$, $Gr = 10^7$; levels $-8.8 \ldots 0.2$ (0.2). Right: temperature field at $\tau = 10$, $Pr = 0.01$, $Gr = 10^7$; levels $0.0 \ldots 1.0$ (0.025)

ACKNOWLEDGEMENTS

This work was supported by the Italian Ministry of Merchant Marine in the frame of INSEAN research plan 1988-90.

REFERENCES

AFRID M, ZEBIB A (1990) Oscillatory Three-Dimensional Convection in Rectangular Cavities and Enclosures. Phys. Fluids A, **2**, 1318

BEHNIA, M and DE VAHL DAVIS, G (1990) Fine Mesh Solutions Using Stream Fuction-Vorticity Formulation. Notes on Num. Fluid Mech., **27**, 11-18.

BEHNIA, M, DE VAHL DAVIS, G, STELLA, F and GUJ, G (1990) A Comparison of Velocity-Vorticity and Stream Function-Vorticity Formulations for Pr = 0. Notes on Num. Fluid Mech., **27**, 19-24.

BRANDT, A (1977) Multi-level Adaptive Solutions to Boundary-Value Problems, Math. Comput., **31**, 333.

ESPOSITO, P G (1991) Numerical Simulation of the Three-Dimensional Lid-Driven Cavity Flow. to appear in the Proc. of the GAMM Workshop on Num. Sim. of 3D Incomp. Unsteady Viscous Lam. Int/Ext Flows, Paris, 1991

KIM, J and MOIN, P (1985) Application of a Fractional Step Method to Incompressible Navier–Stokes Equations. J. Comput. Phys., **59**, 309.

LANGLOIS, W E (1985) Buoyancy-Driven Flows in Crystal-Growths melts. Ann. Rev. Fluid Mech. bf 17, 191-215.

LE QUERÉ, P (1990) A Note on Multiple and Unsteady Solutions in Two-Dimensional Convection in a Tall Cavity. CNRS-LIMSI, Report 90-1, Orsay, France.

MOHAMAD, A A and VISKANTA, R (1991) Transient Natural Convection of Low-Prandtl-Number Fluids in a Differentially Heated Cavity. Int. J. Numer. Meth. Fluids, **13**, 61.

ROUX, B (Editor) (1990) Numerical Simulation of Oscillatory Convection in Low-Pr Fluids. Notes on Num. Fluid Mech., **27**, Viewog Publishers.

WRAY, A A (1987) Very Low Storage Time Advancement Scheme, Private Communication, NASA Ames Research Center.

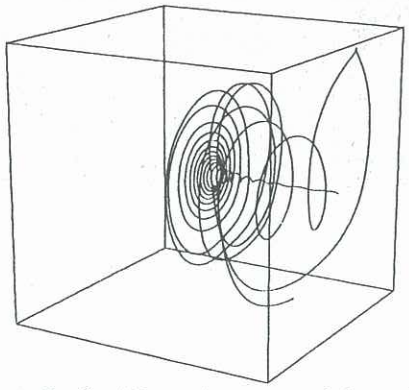

Figure 9: Particle tracks generated from the velocity field at $\tau = 13$. (strating point: 0.5, 0.995, 0.5); $Pr = 0.001$, $Gr = 10^6$

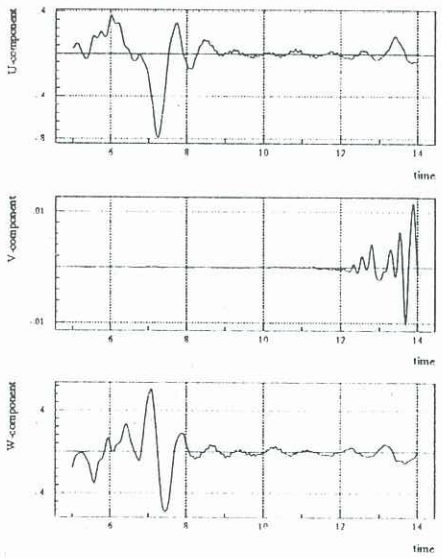

Figure 10: Time history of the velocity components at the centre of the cavity; $Pr = 0.001$, $Gr = 10^6$

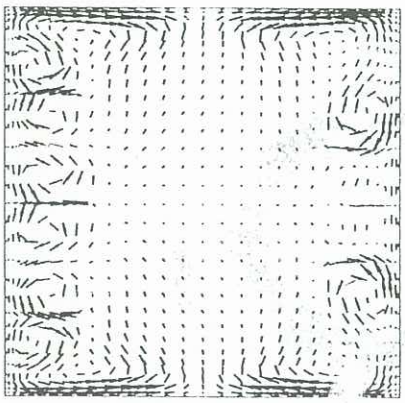

Figure 8: Velocity vectors in the plane $z = 0.5$; $\tau = 13$, $Pr = 0.001$, $Gr = 10^6$

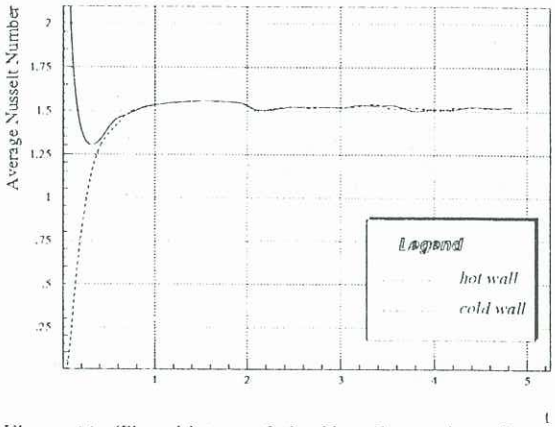

Figure 11: Time history of the Nusselt number: $Pr = 0.01$, $Gr = 10^6$